

## GROUND MOTION STUDIES WITH RESPECT TO LINAC PERFORMANCE

Andrey SERY\*

Commissariat à l’Energie Atomique, DSM/DAPNIA  
 Saclay, F-91191 Gif-sur-Yvette Cedex, France

### Abstract

The future TeV linear collider should have extremely small beam emittance to achieve the required luminosity. Precise alignment of focusing and accelerating elements is necessary to prevent emittance dilution. Analysis of ground motion is therefore an essential problem. This paper reviews studies of ground motion, focusing on the effects the in main linac. After recalling results of measurements of ground motion collected at different places, the method based on spectral description of ground motion, which allows prediction of emittance dilution, in presence of orbit correction feedback as well, is discussed.

### Introduction

The first study of ground motion with respect to linear collider was performed at SLAC by G. Fischer [1]. The intention to build TeV linear collider has inspired new studies started at Protvino [2] and since then in all laboratories developing linear collider projects [3]-[7].

The level of understanding of ground motion has been developed significantly in recent years. The correlation properties of high frequency motion have been investigated [2, 3, 7] in addition to simple spectral amplitude analysis. The slow motion investigations have resulted in discovering of the diffusive ground motion (‘ATL law’ [2]). Dependence of motion on the earth structure was studied [12, 6].

The mathematics, which allows prediction of the effect on the beam, was also being developed in parallel to measurements. The 2-D power spectrum  $P(\omega, k)$ , introduced for ground motion description [4, 8], makes the evaluation of the effect on the beam easy and natural — once this spectrum, the spectral response function of the focusing structure and the spectral properties of applied orbit correction feedbacks are known. The measured data were used to find an approximation of  $P(\omega, k)$  [8] for typical seismic conditions.

This paper intends to show the complete way from measurements to the beam emittance growth. We start from general equations, then consider measured data, create approximation of the 2-D spectrum, and get results using spectral response functions and feedback properties. The misalignment generated beam offset and dispersion in the main regular linac governed by the ‘one to one’ orbit correction is used to illustrate our considerations.

### Linac and Ground Motion

#### General equations

Misalignments of focusing quadrupoles of the linac produce offset of the beam trajectory and hence chromatic dilution of the beam, which can be expressed via an integral involving the power spectrum of the quadrupole displacements and a spectral response function of the considered linac.

Let  $x_i(t) = x(t, s_i)$  be the transverse position of quadrupoles of the linac, relatively to a reference line,  $s_i$  the longitudinal position. The incoming beam angle and position are zero, the reference line passes through some element, placed at the entrance. The beam offset at the exit, relative to the exit position  $x_{fin}$ , and the dispersion, linear term, are

$$x^*(t) = \sum_{i=1}^N c_i x_i(t) - x_{fin} \quad \text{and} \quad \eta_x(t) = \sum_{i=1}^N d_i x_i(t)$$

Here  $c_i$  and  $d_i$  are the first derivatives of the beam offset and dispersion at the exit of the linac with respect to the displacement of the  $i$ -th quadrupole.

While  $\langle x^*(t) \rangle$  and  $\langle \eta_x(t) \rangle$ , averaged on realizations, are zero, the mean squared value gives the offset or dispersive error, for example

$$\langle \eta_x^2(t) \rangle = \sum_i \sum_j d_i d_j \langle x_i(t) x_j(t) \rangle$$

As we consider random process, one can express this through the corresponding power spectrum  $P(t, k)$ .

For initial misalignment or (and) ground motion all spatial harmonics are independent. We have then

$$\langle \eta_x^2(t) \rangle = \int_{-\infty}^{\infty} P(t, k) G_\eta(k) \frac{dk}{2\pi}$$

Here  $G_\eta(k)$  is the so called spectral response function corresponding to dispersion. The expression for the offset is similar, with  $G_{off}(k)$ . The expression allows to obtain results for any spectrum, including the particular case of static gaussian misalignments studied in detail [9].

The spatial power spectrum  $P(t, k)$  of displacements  $x(t, s)$  can be easily found as far as initial misalignment or ground motion are concerned. Assuming that focusing elements are aligned at  $t = 0$  and then are moved by ground motion, the evolution of the power spectrum is [4]:

$$P(t, k) = \int_{-\infty}^{\infty} P(\omega, k) 2 [1 - \cos(\omega t)] \frac{d\omega}{2\pi}$$

It is connected therefore to the 2-D power spectrum  $P(\omega, k)$ , which characterizes ground motion properties, including both spatial and temporal correlation information.

In a regular linac the correction procedures can also be correctly considered within the analytical spectral approach. Correction procedures, such as ‘one to one’ or ‘adaptive alignment’

---

\* On leave from Branch of the Institute of Nuclear Physics, 142284 Protvino, Moscow region, Russia

[10] may introduce correlation of phases between harmonics  $k$  and  $\tilde{k} = k_{\max} - k$  (where  $k_{\max} = \pi/L$ ,  $L$  is the quadrupole spacing). The rms dispersion is then given by an expression, which takes the correlation into account [14].

In short, the spectral response functions  $G(k)$  describe the properties of the focusing channel, while the power spectrum  $P(t, k)$  depends on the applied method of correction, initial misalignment and ground motion.

### Ground motion properties

The 2-D spectrum  $P(\omega, k)$  is hard to measure directly. But if one knows the power spectra of absolute motion and correlation information, or the power spectra of relative motion  $\rho(\omega, L)$ , the 2-D spectrum can be found using

$$\rho(\omega, L) = \int_{-\infty}^{\infty} P(\omega, k) 2 [1 - \cos(kL)] \frac{dk}{2\pi}$$

and the reverse relation [4]. Naturally,  $\rho(\omega, \infty) = 2p(\omega)$ . The measurable correlation, defined via mutual spectrum as  $C(\omega, L) = p_{12}/\sqrt{p_1 p_2}$ , connected to the relative spectrum as  $C(\omega, L) = 1 - \rho(\omega, L)/(2p(\omega))$ .

The power spectrum  $p(\omega)$  of absolute ground motion (which contains contribution of all  $k$ ) grows very fast with decreasing frequency. In quiet conditions it behaves approximately as  $p(\omega) \propto 1/\omega^4$  in rather wide frequency band. The motion is unavoidable as it consists of seismic activity. At low frequency  $f < 1$  Hz the sources are also the atmospheric activity, water motion in the oceans, temperature variations etc. A famous example of the ocean influence is the peak in the band 0.1 – 0.2 Hz with a few micrometers amplitude (Fig.1). In general, motion in the low frequency band  $f < 1$  Hz depend not only on the local conditions, remote sources give significant contribution to the slow motion.

From the other side, in the band  $f > 1$  Hz the human produced noises are usually dominating over the natural noises and the power spectrum depends very much on the local conditions (location of sources, depth of tunnel etc.). Locally generated noises can be much bigger than remotely generated. For example the spectrum measured at the tunnel of operating accelerator (like HERA collider at DESY or SLC at SLAC) presents high amplitudes at  $f > 1$  Hz due to noises generated by different technical devices (Fig.2). These noises may have big amplitude and bad correlation. Technical devices therefore should be properly designed in order to pass as low vibration as possible to the tunnel floor.

It is known from correlation measurements [3, 7] that in quiet conditions the motion in the band  $f > 0.1$  Hz can be considered as wave-like, i.e. the frequency  $\omega$  and wave number  $k$  are connected via phase velocity  $v$ . At  $f \approx 0.1$  Hz the value of  $v$  was found to be close to the velocity of sound (in the surrounding media): about 3000 m/s at LEP and about 2000 m/s at SLC tunnel. At the cultural noise dominated band this value decreases rapidly — the fitted value of  $v$  determined from the measured at SLAC correlation behave as  $v \approx 450 + 1900 \exp(-f/2)$  m/s ( $f > 0.1$  Hz) [7]. The SLAC measurements, which used the most accurate probes, have shown (at least at this place and these

conditions) that contribution of non-wave motion, if there is any not resolved by probes, is negligible at  $f > 0.1$  Hz.

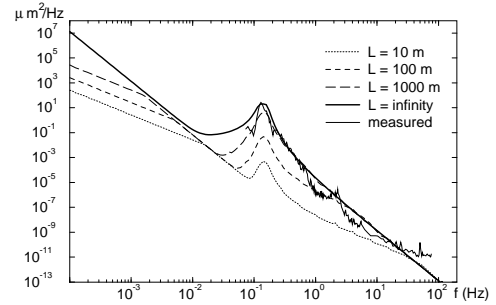


Figure 1: Absolute power spectrum measured in a quiet place (CERN [3]) and the modeling spectrum. Modeling relative spectra  $\rho(\omega, L)$  for different  $L$ .

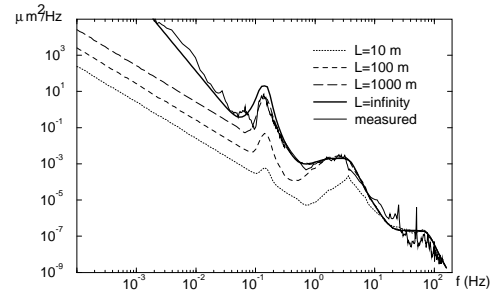


Figure 2: Absolute power spectrum measured in a noisy place (HERA [5]) and the modeling spectrum. Modeling relative spectra for different  $L$ .

The motion at  $f < 0.1$  Hz is different. The elastic motion (produced by the moon, for example) presents here too, but of much bigger relevance is the inelastic diffusive motion, probably fed by the elastic motion and caused by its dissipation. The motion is believed to be described by the ‘ATL law’ [2], which says that the relative rms displacement after a time  $T$  of the two points separated by a distance  $L$  is  $\langle \Delta X^2 \rangle = ATL$ . The parameter  $A$  was found to be  $A \approx 10^{-5 \pm 1} \mu\text{m}^2\text{s}^{-1}\text{m}^{-1}$  for different places. One can see that this displacement is proportional to the square root of the time and separation: this stresses the random, non wavelike, diffusion character of the slow relative motion and means that the number of step-like breaks that appear between two points is proportional to the distance between them and the elapsed time.

If this phenomenon is indeed connected with dissipation of the elastic motion, the parameter  $A$  should depend mainly on the earth properties, because the sources of elastic motion are the same for all places. One could expect that in the places with smaller dissipation the value  $A$  should be smaller and it should also depend on the level of the rock fragmentation. Indeed, the parameter  $A$  was observed to be smaller in tunnels built in solid rock. It also depends on the method of tunnel construction: in the tunnel bored in granite  $A \approx 10^{-6} \mu\text{m}^2\text{s}^{-1}\text{m}^{-1}$  was observed, while in the similar tunnel, which was built by use of explosions, the parameter  $A$  is found to be 5 times larger probably because of the fragmentation, artificially increased during construction [6].

The parameter  $A$  also depends on the tunnel depth, generally it is smaller in deeper tunnels [12].

The ranges of  $T$  and  $L$  where the ‘ATL law’ is valid are very wide. In [12] it was summarized that ‘ATL’ is confirmed by measurements of ground motion in different accelerator tunnels in the range from minutes to tens of years and from a few meters to tens of kilometers. The measured relative power spectra, presented in [6] and in [11], exhibit the ‘ATL’ behavior already for  $f < 0.1$  Hz (for  $L \approx 30$  m). These measurements indicate that the transition region from wave to diffusion motion is placed at rather short times (a few seconds). This can result in certain decreasing of correlation around  $f \propto 0.01$  Hz.

Although the ‘ATL law’ was found from the direct analysis of measurements of ground motion, its most interesting confirmations come from the observations of beam motion in big accelerators produced by displacements of the focusing elements. An example is the measurements of the closed orbit motion in the HERA circular collider, which have shown that the power spectrum of this motion corresponds to the ‘ATL law’ in a wide frequency range, from  $f \approx 0.1$  Hz down to  $f \approx 10^{-6}$  Hz [11].

The very slow motion can be systematic (not described by power spectrum) as well. Such motion has been observed at LEP Point 1 and PEP [13] where some quadrupoles move unidirectionally during many years with rate about  $0.1 - 1$  mm/year. Quite close (a few tens of meters) points can move in opposite direction. Amplitude of the motion can be larger than the one of diffusive motion. The motion is probably due to geological peculiarities of the place or due to relaxation if the tunnel was bored in solid rock.

Ending with the ground motion one could note that the elements of the linac will be placed not on the floor, but on some girder, which could amplify some frequencies due to its own resonances. It is not only this amplification that is dangerous, more important is that the not identical girders will amplify or change the floor motion by different way, which can spoil correlation of the floor motion. It is therefore preferable to push the girder resonances to high frequencies where the correlation is poor anyway and floor amplitudes are smaller. This requires firm connection of the girder with the floor. The active systems [15], which can help in certain extend to isolate the quadrupoles from high frequency human induced floor motion, should be made insensitive to slow motion (say, below 1 Hz), otherwise long wavelength motion can create more dangerous short wavelength due to inequality of active supports.

### Ground motion model

The approximation for  $P(\omega, k)$  is built [8] in assumption that the low frequency part of motion is described by the ‘ATL law’, while the high frequency part is produced mainly by waves. The 2-D spectrum corresponded the ‘ATL’ motion is  $P(\omega, k) = A/(\omega^2 k^2)$  (here  $\omega$  and  $k$  are defined on the entire axis). In order to be included into the model, this spectrum should be corrected because it overestimates fast motion — the corresponded spectrum of relative motion exceeds the one of absolute motion. The correction is made by the way that will overestimate the effect rather than underestimate it. Better model

can be built once measured data on transition region are available. The elastic waves are assumed to be transverse, propagating at the surface of the ground with uniform distribution over azimuthal angle. Finally, the modeling spectrum is:

$$P(\omega, k) = \frac{A}{\omega^2 k^2} (1 - \cos(kB/A/\omega^2)) + \sum_i D_i(\omega) U_i(\omega, k)$$

The function  $U_i(\omega, k)$  describes the wave number distribution of the waves with frequency  $\omega$ . In our case  $U_i(\omega, k) = 2/\sqrt{k_{\text{cut}}^2 - k^2}$  if  $|k| \leq k_{\text{cut}}$  and zero otherwise. Here  $k_{\text{cut}}(\omega) = \omega/v_i$  and  $v_i$  the phase velocity of wave propagation. The cases  $k = 0$  and  $k = k_{\text{cut}}$  correspond to the waves propagating perpendicular and along the linear collider correspondingly. Since the integral over  $dk/(2\pi)$  of  $U(\omega, k)$  equals one, the function  $D(\omega)$  describes contribution of these waves to the absolute spectrum  $p(\omega)$ . We write  $D(\omega)$  as  $D_i(\omega) = a_i/(1 + [d_i(\omega - \omega_i)/\omega_i]^4)$ . In order to model complex behavior of the spectrum, for example in presence of cultural noises, a few terms with waves added to  $P(\omega, k)$ ,  $i$  is the number of the peak.

We consider here two models. Parameters of the first model are the following:  $A = 10^{-5} \mu\text{m}^2\text{s}^{-1}\text{m}^{-1}$ ,  $B = 10^{-6} \mu\text{m}^2\text{s}^{-3}$ . The single peak described by  $\omega_1 = 2\pi \cdot 0.14$  Hz for the frequency of the peak,  $a_1 = 10 \mu\text{m}^2/\text{Hz}$  for its amplitude,  $d_1 = 5$  for its width, and  $v_1 = 1000$  m/s for the velocity. It is the model of quiet place such as LEP tunnel during shutdown. The thick line on Fig.1 shows the spectrum of absolute motion, calculated from  $P(\omega, k)$ , corresponding to these parameters. The actual measured  $p(\omega)$  can be bigger than the modeling one at  $f < 0.1$  Hz, because slow long wavelength motion does not included into the model. The second model corresponds to seismic conditions with big contributions from cultural noises (as in the HERA tunnel in operating conditions). The parameters are the following:  $A = 10^{-5} \mu\text{m}^2\text{s}^{-1}\text{m}^{-1}$ ,  $B = 10^{-3} \mu\text{m}^2\text{s}^{-3}$  and three peaks:  $f_1 = 0.14$ ,  $f_2 = 2.5$ ,  $f_3 = 50$  Hz;  $a_1 = 10$ ,  $a_2 = 10^{-3}$ ,  $a_3 = 10^{-7} \mu\text{m}^2/\text{Hz}$ ;  $d_1 = 5$ ,  $d_2 = 1.5$ ,  $d_3 = 1.5$ ;  $v_1 = 1000$ ,  $v_2 = 400$ ,  $v_3 = 400$  m/s. One can see (Fig.3) how the waves are faded by the ‘ATL’ in  $P(t, k)$  when time increases. The parameters of these two models have been chosen taking into account correlation measurements in the LEP [3], HERA [5] and SLC [7] tunnels and measurements of the closed orbit motion in HERA [11].

The effect of the ground motion on the beam can be obtained both by analytical way via the integral of spectral function with the modeling power spectrum and also by simulations, when ground motion displacement  $x(t, s)$  is modeled by summation of harmonics and the beam degradation determined by particle tracking. In the latter case we first analyze the modeling  $P(\omega, k)$  spectrum to define the band of relevant  $\omega$  and  $k$ , assuming that  $T_{\text{min}} < T < T_{\text{max}}$  and  $L_{\text{min}} < L < L_{\text{max}}$ . Then we split this 2-D band by cells ( $50 \times 50$  typically) equidistantly in logarithmic sense, find rms amplitude of each cell  $a_{ij}$  and generate two sets of random phases  $\phi_{ij}$  and  $\psi_{ij}$ . Positions of  $\omega_i$  and  $k_j$  within each cells are chosen randomly so after many seeds all  $(\omega, k)$  will be checked. The modeling displacement  $x(t, s)$  is then

$$x(t, s) = \sum_i \sum_j a_{ij} [\sin(\omega_i t) \sin(k_j s + \phi_{ij}) + (\cos(\omega_i t) - 1) \sin(k_j s + \psi_{ij})]$$

This harmonics model was used in our simulations, eventually it will be used in the linear collider flight simulator ‘MERLIN’ [16], which is being developed to analyze performance of the beam delivery systems.

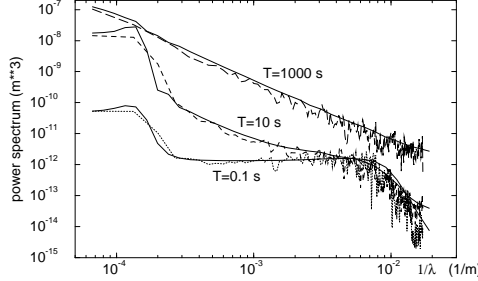


Figure 3: Modeling power spectra  $P(t, k)$  for the second noisy model and the spectra obtained in simulations using the harmonics model.

### Spectral response function

The spectral response function corresponded to dispersion of the beam is

$$G_{\eta}(k) = \left( \sum_{i=1}^N d_i (\cos(ks_i) - 1) \right)^2 + \left( \sum_{i=1}^N d_i \sin(ks_i) \right)^2$$

Similar for the offset, with  $c_i$ , with the sum runs up to  $N + 1$  and  $c_{N+1} = -1$ . In thin lens approximation, in linear order  $c_i = -K_i r_{12}^i$  and  $d_i = K_i (r_{12}^i - t_{126}^i)$  where  $K_i$  is  $r_{21}$  of the quadrupole matrix,  $r_{12}^i$  and  $t_{126}^i$  are the matrix elements from the  $i$ -th quadrupole to the exit.

At small  $k$  one has  $G_{\text{off}}(k) \approx k^2 R_{12}^2$  and  $G_{\eta}(k) \approx k^2 T_{126}^2$ . For the regular linac only the band  $[0, k_{\text{max}}]$  is unique. In this band the spectral function has two resonances:  $kL = \mu/2$  and  $kL = \pi - \mu/2$ . The values of spectral function at these resonances as well as their width can be found analytically.

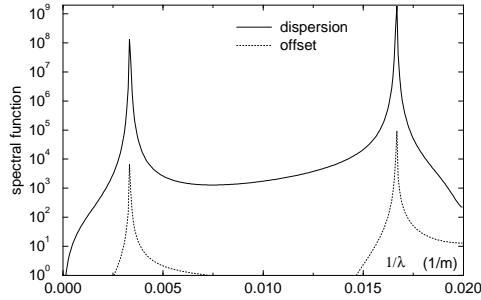


Figure 4: Spectral response functions.

The examples in this paper are given for the modeling FODO linac: number of quadrupoles  $N = 600$ , spacing  $L = 25$  m, phase advance  $\mu = 60$  degrees, initial and final energy  $\gamma_{\text{ini}} = 6000$ ,  $\gamma_{\text{fin}} = 5 \cdot 10^5$ , beta functions at the even defocusing quadrupoles and at the exit are  $\beta_{\text{min}} = 28.86$  m. The spectral functions for this linac are shown on Fig.4.

### Free evolution

Fig.5 shows the rms beam offset relative to the linac exit versus time for quiet and noisy models of ground motion. The an-

alytical results are shown in comparing with results of simulations, which use tracking and the model of harmonics to simulate beam line misalignment. To estimate the critical time scale, this offset should be compared with the beam size at the exit. If  $\gamma \varepsilon_y = 2.5 \cdot 10^{-7}$  m, then at the exit  $\sigma_y \approx 3.5 \cdot 10^{-6}$  m and the critical time is about one minute. For somewhat smaller emittance the cultural noise of the second model becomes important and the critical time decreases to a fraction of second.

One can see that the chosen  $P(\omega, k)$  spectrum gives a linear dependence of the relative misalignment variance (and hence the rms beam offset as well) versus time for large  $T$  (‘ATL’ behavior), while for small  $T$  the variance is proportional to  $T^2$ . This square dependence at small time is the general property of the spectrum that drops fast enough with increasing frequency [17]. One can mention that if the systematic motion is significant, the  $T^2$  behavior will appear at big  $T$  too.

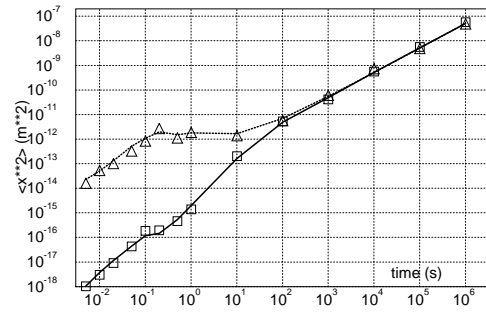


Figure 5: Relative beam offset. Free evolution. Quiet and noisy models. Analytical results (lines) and simulations.

### Feedback controlled evolution

Many feedbacks will inevitably be used in linear collider. To study the equilibrium rms offset accurately, one need to put the feedback gain function into the integral, which will suppress frequencies smaller than  $f_{\text{rep}}/6 - f_{\text{rep}}/20$ .

To illustrate influence of an orbit correction feedback on the beam dispersion, let us consider the ‘one-to-one’ algorithm, which consists in zeroing the BPM measurements (assumed to be perfect). Here we assume that this is done by steering the beam by means of dipole correctors (equivalent to the quadrupole shift). This and other orbit correction or alignment methods are considered in more details (including BPM errors etc.) elsewhere [14].

If the  $i$ -th quadrupole is misaligned, three angles are needed to re-align the beam. The equivalent quadrupole displacements, to be subtracted from their initial positions, are (if acceleration is neglected):

$$\Delta x_i = -2x_i/(LK_i), \quad \Delta x_{i+1} = \Delta x_{i-1} = -x_i/(LK_i)$$

After such a procedure the beam trajectory will pass through positions of quadrupoles before correction (Fig.6).

To find the beam dispersion one can notice that in spectral approach, in a regular FODO lattice with  $K_i = -K_{i+1}$ , a  $k$ -th harmonics of the initial misalignment produces two harmonics of quadrupole displacements after the correction:  $k$ -th and  $(k_{\text{max}} - k)$ -th with opposite phases. If this self correlation as

well as injection conditions are taken into account, the dispersion after correction can be found [14].

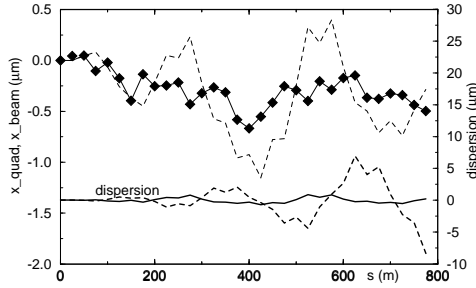


Figure 6: Position of quadrupoles (symbols) before correction, beam trajectories (lines) and dispersion before and after correction. Quiet model at  $t = 100$  s.

An alternative way to write the beam dispersion after ‘one-to-one’ correction is

$$\langle \eta_x^2(t) \rangle = 2 \int_0^{k_{\max}} \hat{P}(t, k) \hat{G}_\eta(k) \frac{dk}{2\pi} \quad (1)$$

where  $\hat{G}_\eta(k)$  and  $\hat{P}(t, k)$  are the effective spectral response function and the effective spectrum of quadrupole displacements before correction (which can include BPM offset and resolution errors also) respectively. The  $\hat{G}_\eta(k)$  is built with new coefficients (neglecting acceleration) [14]:

$$\hat{d}_i = d_i + (2d_i + d_{i+1} + d_{i-1}) / (LK_i)$$

It gives  $\hat{d}_i = -K_i r_{12}^i$ . This follows from the algorithm of correction — the angle caused by displaced quadrupole is corrected, thus the term  $T_{126}$  vanishes. The  $\hat{G}_\eta$  and  $G_{\text{off}}$  are practically the same therefore. The considered ‘one-to-one’ scheme reduce emittance growth by factor  $N^2$  roughly, which increase significantly the time interval until a beam based alignment might be again required. The critical time (when  $\Delta p/p\eta = \sigma_y$ ) for the beam with  $\Delta p/p = 10^{-3}$  is a few hours without and about one year with correction (Fig.7).

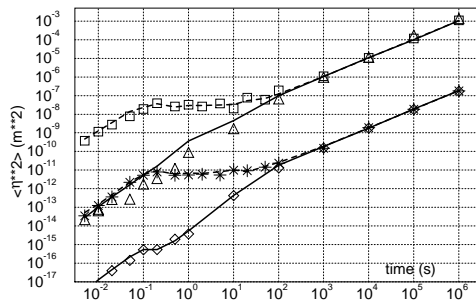


Figure 7: Beam dispersion. Free (upper curves) and feedback controlled evolution (lower curves).

Fig.7 shows dispersion without and with ‘one-to-one’ correction. In the second case the dispersion is shown at the moment just after correction. This value does not depend on how many times the correction has been applied before. If the repetition rate of corrections is enough high, the values just after and just before correction are very close.

### Conclusion

A future TeV linear collider, having extremely small emittance of beams, will suffer from the ground motion, which will spoil alignment of focusing and accelerating elements and result in offset and emittance growth.

The ground motion studies, performed by different laboratories, resulted in significant improvement of understanding of this phenomenon. Different types of motion have been investigated, many factors that the motion depends on are learned. The mathematical formalism allowing prediction of the beam behavior is developed.

Though many ground motion features are still to be carefully investigated, one may reasonably believe that the ground motion problem of the future linear collider can be overcome provided that stored knowledge will be used at each step of design and construction.

### Acknowledgement

I am grateful to colleagues from Novosibirsk INP and Protvino Branch INP for being working together over many years and to colleagues from CERN, DESY, CEA Saclay and SEFT for fruitful collaborations. I am indebted to colleagues from KEK and SLAC for numerous helpful discussions.

### References

- [1] G. E. Fischer, SLAC-PUB-3392 Rev., 1985.
- [2] B. Baklakov, P. Lebedev, V. Parkhomchuk, A. Sery, A. Sleptsov, V. Shiltsev, INP 91-15; Tech. Ph. **38**, 894, (1993).
- [3] V. Juravlev, A. Sery, A. Sleptsov, W. Coosemans, G. Ramseier, I. Wilson, CERN SL/93-53, CLIC-Note 217, 1993.
- [4] V. Juravlev, P. Lunev, A. Sery, A. Sleptsov, K. Honkavaara, R. Orava, E. Pietarinen, HU-SEFT R 1995-01, Helsinki 1995.
- [5] V. Shiltsev, B. Baklakov, P. Lebedev, J. Rossbach, C. Montag, DESY HERA 95-06, June 1995.
- [6] Shigeru Takeda, K. Kudo, A. Akiyama, Y. Takeuchi, T. Katoh, Y. Kanazawa, S. Suzuki, Proc. EPAC 96, 1996.
- [7] C. Adolphsen, G. Mazaheri, T. Slaton, in Proc. of Workshop on Physics and Experiments with Linear Colliders, Tsukuba, 1995; Zeroth Order Design Report for the NLC, SLAC, 1996.
- [8] A. Sery, O. Napoly, Phys. Rev. E. **53**, 5323, (1996).
- [9] T. O. Raubenheimer, SLAC report 387, 1991.
- [10] V. Balakin, in Proc. of Workshop on Next Generation Linear Collider LC91, Protvino, 1991.
- [11] R. Brinkmann, J. Rossbach, Nucl.Instr.Meth.A **350**, 8, (1994).
- [12] V. Shiltsev, in Proc. of Workshop on Accelerator Alignment, Tsukuba, 1995.
- [13] R. Pitthan, SLAC-PUB 95-7043, 1995.
- [14] A. Sery, A. Mosnier, DAPNIA/SEA/96-06, CEA Saclay, 1996.
- [15] C. Montag, DESY 96-053, 1996.
- [16] N. J. Walker, work in progress.
- [17] S. Fartoukh, O. Napoly, A. Sery, DAPNIA/SEA/95-05, CEA Saclay, 1995.